BASIC SCIENCE

Nanomedicine: Nanotechnology, Biology, and Medicine
20 (2019) 102014

Original Article

nanomedjournal.com

Interfering with endolysosomal trafficking enhances release of bioactive exosomes

Francisco G. Ortega, PhD[a], Marieke T. Roefs, MSc[b], Diego de Miguel Perez, MSc[c,d], Sander A. Kooijmans, PhD[a], Olivier G. de Jong, PhD[a], Joost P. Sluijter, PhD[b,e], Raymond M. Schiffelers, PhD[a], Pieter Vader, PhD[a,b,*]

[a]*Laboratory of Clinical Chemistry and Haematology, University Medical Center Utrecht, Utrecht, The Netherlands*
[b]*Department of Cardiology, Laboratory of Experimental Cardiology, University Medical Center Utrecht, Utrecht, The Netherlands*
[c]*Liquid Biopsy and Metastasis Research Group, GENYO, Centre for Genomics and Oncological Research, Pfizer/University of Granada/Andalusian Regional Government PTS, Granada, Granada, Spain*
[d]*Laboratory of Genetic Identification, Legal Medicine and Toxicology Department, Faculty of Medicine, University of Granada, Granada, Spain*
[e]*Regenerative Medicine Center Utrecht, University Medical Center Utrecht, Utrecht, The Netherlands*

Revised 15 April 2019

Abstract

Exosomes are cell-derived extracellular vesicles of 30-150 nm in size and are involved in intercellular communication. Because of their bioactive cargo, consisting of proteins, RNA and lipids, and their natural ability to deliver these biomolecules to recipient cells, exosomes are increasingly being studied as novel drug delivery vehicles or as cell-free approaches to regenerative medicine. However, one of the major hurdles for clinical translation of therapeutic strategies based on exosomes is their low yield when produced under standard culture conditions. Exosomes are vesicles of endocytic origin and are released when multivesicular endosomes fuse with the plasma membrane. Here, we demonstrate that interfering with endolysosomal trafficking significantly increases exosome release. Furthermore, these exosomes retain their regenerative bioactivity as demonstrated by pro-survival and angiogenesis assays using both cardiomyocytes and endothelial cells. These results may be employed to increase exosome production for studying biological functions or to improve clinical translation of exosome-based therapeutics.

Key words: Exosomes; Vesicle biogenesis; Extracellular vesicles; Endolysosomal trafficking; Exosome functionality; Regenerative medicine

Exosomes are small extracellular vesicles between 30 and 150 nm in size and are produced by all cells in the human body. They originate from multivesicular endosomes (MVEs) and are released through the fusion of these MVEs with the plasma membrane.[1] This distinct intracellular origin discriminates exosomes from other extracellular vesicles, such as microvesicles or ectosomes, which are generated by outward budding of the plasma membrane, and are typically larger (100 to 1000 nm) in size.

Exosomes carry biological cargo derived from the donor cell, including proteins, RNA (both coding and non-coding), and lipids. Through horizontal transfer of these bioactive cargoes, exosomes have been demonstrated to play an important role in cell–cell communication,[2–4] affecting the behavior of proximal and/or distal target cells throughout the body[5,6] in a target-specific manner. For instance, it has been shown that exosomes are involved in biological processes including maturation of erythrocytes,[7] antigen presentation in immune responses,[8]

FO thanks Fundación Ramón Areces for supporting him through a study abroad postdoctoral program. JS, MR, and PV are supported by H2020 ERC-2016-COG EVICARE (725229). PV is supported by a VENI Fellowship from the Netherlands Organization for Scientific Research (NWO). George Posthuma is gratefully acknowledged for technical assistance in electron microscopy experiments.

Conflict of Interest: None declared.

*Corresponding author at: Department of Clinical Chemistry and Haematology & Laboratory of Experimental Cardiology, University Medical Center Utrecht, 3584 CX, Utrecht, The Netherlands.

E-mail address: pvader@umcutrecht.nl. (P. Vader).

https://doi.org/10.1016/j.nano.2019.102014

Please cite this article as: Ortega FG, et al, Interfering with endolysosomal trafficking enhances release of bioactive exosomes. *Nanomedicine: NBM* 2019;20:102014, https://doi.org/10.1016/j.nano.2019.102014

coagulation,[9] inflammation,[10] and angiogenesis.[11] Besides these physiological processes, exosomes have also been found to be involved in many pathological processes such as cancer,[12] Parkinson's disease,[13] myocardial infarction[14]and human immune deficiency virus infection.[15]

Since the discovery that exosomes are natural delivery systems of biological molecules, the scientific community has been evaluating exosomes for the treatment of different kinds of injuries and diseases. For example, exosomes from different cell types have been employed for delivery of various therapeutic molecules,[16–19] while exosomes derived from stem cells or progenitor cells have intrinsic therapeutic potential for regenerative medicine applications by virtue of their endogenous bioactive cargo.[10,20–24] Unfortunately, one of the limitations of therapeutic strategies based on exosomes is their low yield when produced under standard culture conditions. Therefore, there is a need to increase exosome yield, while maintaining their functionality.[17,25]

Exosome biogenesis occurs during the process of endosomal maturation. In general terms, this process begins with endocytosis and ends with the degradation of the endosomal content by fusion of late endosomes with lysosomes.[26] During this process, small endocytic vesicles fuse to form larger early endocytic vesicles, while the pH of these vesicles is reduced progressively and the formation of intraluminal vesicles (ILVs) commences.[27,28] Subsequently, during endosomal maturation, endosomes no longer fuse with small endocytic vesicles. As the pH is further reduced, the formation of ILVs is significantly more evident.[29] These multivesicular endosomes are also called late endosomes or multivesicular bodies. At this point, intraluminal vesicles can be degraded by lysosomes or released to the extracellular environment as exosomes. Interestingly, it has been described that inhibition of lysosomal function prevents endosome maturation, leading to accumulation of ILVs in MVEs.[30]

Here, we set out to evaluate whether interfering with endolysosomal trafficking through inhibition of endosomal maturation and/or reduction of lysosomal function increases release of exosomes, and whether these exosomes retain their bioactive properties.

Methods

Cell culture

Cells were grown in Dulbecco's Modified Eagle Medium (DMEM) (Gibco™, USA) supplemented with 10% fetal bovine serum (FBS) and penicillin/streptomycin (100 U/ml and 100 μg/ml, respectively). Cardiac progenitor cells (CPCs), human microvascular endothelial cells (HMEC-1) and HL-1 cells were grown on 0.1% gelatin-coated surfaces. CPCs were grown in EGM-2 medium (EBM-2 supplemented with growth medium-2 BulletKit™, 30 μg/ml gentamicin and 15 ng/ml amphotericin) (LONZA, USA):M199 medium (Gibco™, USA) (1:3), supplemented with 10% FBS, penicillin/streptomycin (100 U/ml and 100 μg/ml, respectively) and 1% non-essential amino acids solution (Sigma, USA).[31] HMEC-1 cells were cultured in MCDB131 medium supplemented with 10% FBS, penicillin/streptomycin (100 U/ml and 100 μg/ml, respectively), epithermal grown factor (10 ng/ml), hydrocortisone (50 nM) and L-Glutamine (2 mM). HL-1 cells were cultured in Claycomb medium (Sigma, USA), supplemented with 10% FBS, 1x GlutaMAX (Gibco™, USA), penicillin/streptomycin (100 U/ml and 100 μg/ml, respectively), ascorbic acid (0.3 mM) and phenylenephrine (0.1 mM). For exosome isolation, MDA-MB-231, HT29 and SKOV3 cells were cultured for 24 h in DMEM without FBS, while CPCs were cultured for 24 h in serum-free M199. All cells were cultured at 37 °C, 5% CO_2 and 20% O_2.

Lentiviral constructs

Two short hairpin (sh) NDRG1 sequences (target sequence 1: CCTGGAGTCCTTCAACAGTTT and sequence 2: GCACATTGTGAATGACATGAA) and two shRAB7 sequences (target sequence 1: GCCACAATAGGAGCTGACTTT and sequence 2: ACGAATTTCCTGAACCTATCA) previously described by Tschan et al[32] and Alonso-Curbelo et al,[33] respectively, were cloned into a pLKO.1 backbone (Addgene, USA). The control lentiviral vector was shLuciferase (target sequence: AAGAGCACTCTCATCGACAAG) in pLKO.1 vector that did not match to any known human gene, and is referred to as shControl. pLKO.1 constructs were transfected together with psPAX2 and pMD2.G vectors at a 2:1:1 ratio using Lipofectamine 2000 into HEK-293T cells. Cells were incubated for 24 h, fresh medium was added, and lentiviral particles were collected every 24 h over the following 48 h. Target cells were infected with 10% of media containing virus and 8 μg/ml hexadimethrine bromide (Polybrene). Media were changed 24 h after infection and puromycin was added to select stable knockdown (KD) cells.

Exosome isolation

Exosomes were isolated from serum-free conditioned media when cells had reached 90%-95% confluency, using serial centrifugation or size exclusion chromatography (SEC) where indicated. Serial centrifugation was performed as previously described.[25] Briefly, conditioned medium was spun at 300 ×*g* for 15 min to remove cell contamination, 2000 ×*g* for 15 min to remove cell debris and 10,000 ×*g* for 30 min to remove larger microvesicles and apoptotic bodies. Finally, supernatant was centrifuged at 120,000 ×*g* for 1 h to obtain an exosome-rich pellet. When indicated, size exclusion chromatography was performed on conditioned media after serial centrifugation of 300 ×*g* for 15 min, 2000 ×*g* for 15 min and 10,000 ×*g* for 30 min as described.[25] Media were concentrated with 100 kDa spin filters (Amicon®, USA) until 5 ml and then injected into a SEC Hiprep™ 16/60 Sephacryl® S-400 HR column (GE Healthcare, USA) at a flow rate of 0.5 ml PBS/min. Aliquots of 5 ml were collected and exosome-containing fractions were employed for further analysis.

Western blot analysis

Cells or exosomes were lysed with RIPA buffer for 15 min on ice and then centrifuged at 12,000 ×*g* for 15 min. Supernatants were collected and employed as protein extract. Protein

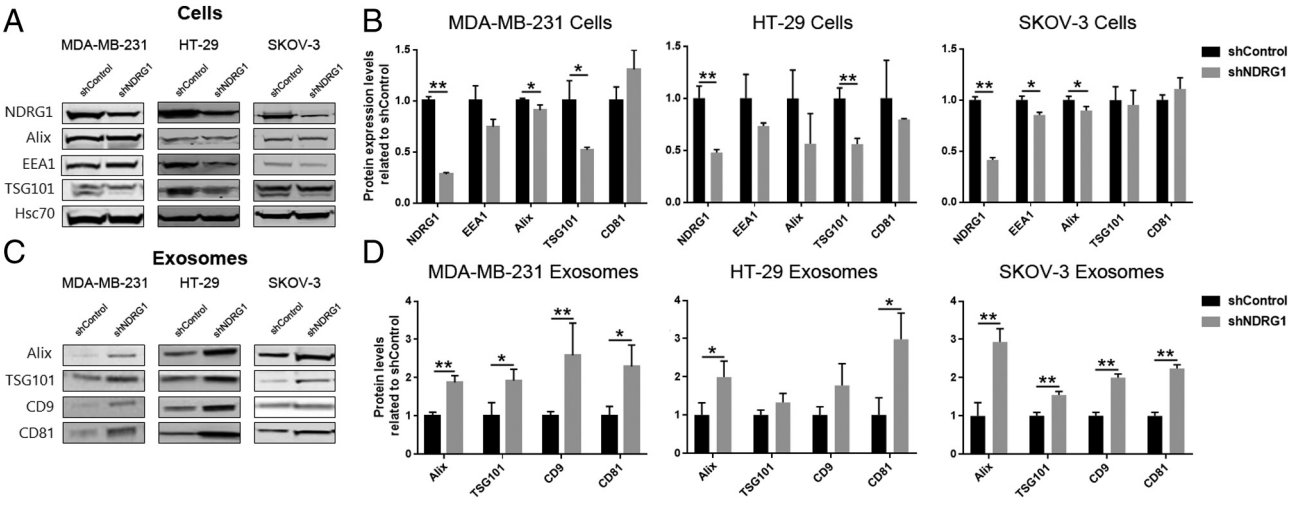

Figure 1. **Knockdown of NDRG1 increases release of exosomal markers. (A, B)** NDRG1, EEA1 and exosomal marker protein levels in NDRG1 KD and shControl cells were analyzed by Western Blot. Equal protein amounts were loaded. **(A)** Representative Western Blot of MDA-MB-231, HT-29 and SKOV-3 cells. **(B)** Quantification of protein levels in NDRG1 KD and shControl cells. Hsc70 was used as a loading control. Band intensities were determined using ImageJ software and normalized to Hsc70. Bars represent mean of three independent experiments relative to the shControl. Error bars show SD and significance is represented as * (P <0.05) or ** (P <0.01) as determined by Student's t test. **(C, D)** Exosomes were isolated by serial centrifugation from 25 ml of media of NDRG1 KD and shControl cells. Exosomal marker protein levels were analyzed by Western Blot. Equal volumes (containing all exosomes isolated from 25 ml of media) were loaded. **(C)** Representative Western Blot of isolated exosomes from MDA-MB-231, HT-29 and SKOV-3 cells. **(D)** Quantification of protein levels in exosomes from NDRG1 KD and shControl cells. Band intensities were determined using ImageJ software and normalized to the average intensity of each protein. Bars represent mean of three independent experiments relative to shControl. Error bars show SD and significance is represented as * (P <0.05) or ** (P <0.005) as determined by Student's t test.

concentrations were quantified using a Pierce microBCA kit (ThermoFisher Scientific, USA) according to the manufacturer's instructions. Proteins were loaded into precast 4%-12% Bis–Tris polyacrylamide gels (ThermoFisher Scientific, USA) and resolved by SDS-PAGE at 100 mA for 90 min. Then, proteins were transferred to a PVDF membrane (BIORAD, USA) at 30 mA overnight. Membranes were blocked with 50% v/v Odyssey® blocking buffer (LI-COR, Germany) in Tris buffered saline (TBS) for 30 min at room temperature and probed overnight at 4 °C with primary antibodies. Finally, membranes were incubated with secondary antibodies labeled with infrared fluorescent dye or HRP conjugated secondary antibodies for 1 h at room temperature. Proteins of interest were visualized using a ChemiDoc MP (BIORAD, USA) or an Odyssey® Imaging system (LI-COR, Germany).

Primary antibodies included anti-CD9 (clone EPR2949), anti-CD63 (clone MEM-259), anti-TSG101 (ab30871) (Abcam, UK), anti-CD81 (clone B-11) (Santa Cruz Biotech, USA), anti-Hsc70 (clone BB70) (Enzo Life Science, Belgium), anti-RAB7 (clone 10E4), anti-NDRG1 (clone JM32-02) (Novus Biological, UK), anti-Alix (clone 3A9) (Themofisher, USA), anti-β-actin (clone AC-15, Sigma, USA), anti-phospho AKT (D9E), anti-AKT (clone 11E7), anti-phospho ERK1/2 (Phospho-p44/42 MAPK (Thr202/204)) and anti-ERK1/2 (p44/42 MAPK) (Cell Signaling, USA). Secondary antibodies included Alexa Fluor 680-conjugated anti-rabbit (A-21076), IRDye 800CW anti-mouse (926-32,212) (LI-COR, Germany) and HRP-conjugated goat anti-rabbit (Dako).

Acridin orange (AO) analysis

Cells grown in 8 wells culture slides (Ibidi, Germany) were incubated with acridine orange (Sigma, USA) (20 nM) for 15 min at 37 °C, washed 3 times with PBS, fixed with a 4% paraformaldehyde/PBS solution and mounted with antifade mounting medium with DAPI (Vectorlabs, UK). Finally, stained samples were examined with a Zeiss LSM confocal microscope using a 40× objective. Images were analyzed with ZEN software.

Transmission electronic microscopy

Exosomes were adsorbed on active-carbon coated grids for 10 min, washed and fixed for 15 min in a 2% paraformaldehyde and 0.2% glutaraldehyde solution. Then, grids were rinsed briefly and immediately transferred to drops of uranyl methyl cellulose pH 4.0 on a cooled metal plate for 5 min, picked up and dried at room temperature. Finally, grids were introduced in a FEI Tecnai™ F20 transmission electron microscope (TEM) and 20 pictures for every biological sample were taken. Pictures were analyzed with ImageJ software[34] by an independent investigator in a double blinded manner.

Phospholipid analysis

Exosomes were lysed by adding 375 µl of 1:2 chloroform/methanol solution. Then, 125 µl of chloroform and 125 µl of ddH2O were added until two clearly separated phases were obtained. Organic phase was collected and employed for inorganic phosphate determination by modified Rouser assay.[35] Briefly, samples and phosphorus standard curves were dried at 180 °C in a heating block. A 0.3 ml 70% perchloric acid solution was added and incubated for 30 min at 180 °C. After cooling, 0.5 ml 1.25% ammonium molybdate solution, 0.5 ml 5% ascorbic acid and 1.0 ml ddH_2O were added. Tubes were

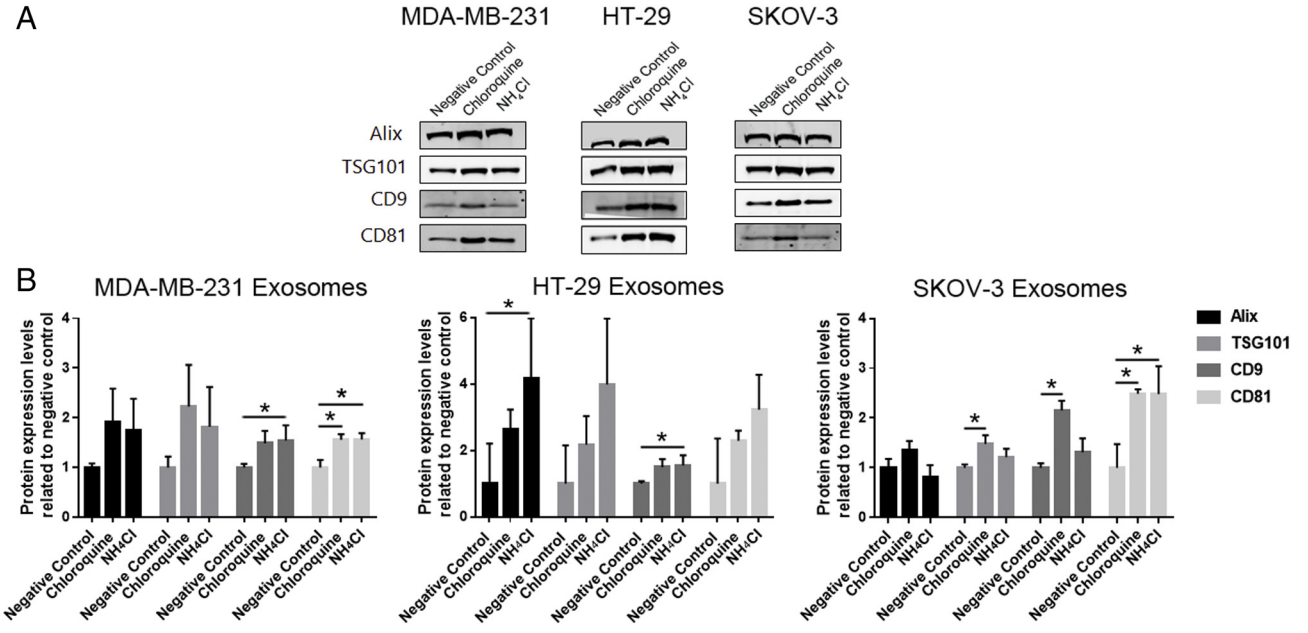

Figure 2. **Chloroquine or NH_4Cl treatment increases release of exosomal markers.** Exosomes from 25 ml media of treated or control cells were isolated by serial centrifugation. Exosomal marker proteins were analyzed by Western Blot. **(A)** Representative Western Blot of isolated exosomes from MDA-MB-231, HT-29 and SKOV-3 cells. **(B)** Quantification of protein levels in exosomes from treated and control cells. Band intensities were determined using ImageJ software. Bars represent mean of three independent experiments relative to negative control. Error bars show SD and significance is represented as * (P <0.05) as determined by one-way ANOVA with Dunnett's multiple comparison test.

incubated in boiling water for 7 min until a colorimetric reaction was observed. Finally, absorbances of samples and standard curves were measured at 830 nm using a spectrophotometer.

Nanoparticle tracking analysis

Exosome size distribution and concentration were measured using a NanoSight NS500 system equipped with an LM14 405 nm violet laser unit (Malvern Instruments, UK). Concentrated exosome samples were diluted with PBS to appropriate dilutions for analysis (generally 1:1000) and visualized at camera level 16 under control of a script, which included acquisition of 3 movies of 1 min at a fixed temperature of 22 °C. Analysis was performed with NTA 3.1 software. Detection threshold was set at 5 and other settings were kept at default.

Determination of AKT and ERK 1/2 phosphorylation

First, 1×10^5 HMEC-1 and HL-1 cells were seeded in 24 well culture plates (Corning, USA). After 24 h, cells were starved in basal MCDB-131 medium for 3 h. Next, cells were stimulated with a fixed number of exosome particles from treated or control CPCs (0, 6.0×10^{10} or 1.2×10^{11} particles) for 30 min, after which cells were lysed using RIPA buffer. Cell lysates were centrifuged for 10 min at 12,000 ×g and supernatants were employed for Western Blot analysis.

Tube formation assay

First, 1×10^5 HMEC-1 cells were seeded in 24 well culture plates. After 6 h, cells were starved in basal MCDB-131 medium and stimulated with a fixed number of exosomes from control or treated CPCs (0, 6.0×10^{10} or 1.2×10^{11} particles) for 12 h. Then, 2×10^3 cells per well were seeded on 10 μl growth factor reduced Matrigel (ThermoFisher Scientific, USA) on angiogenesis μ-slides (Ibidi, Germany) in MCDB-131 medium in the presence of exosomes. After 7 h, pictures were taken using a Olympus BX53 microscope equipped with a CCD (DP71, Olympus) camera and analyzed by the angiogenesis analyzer tool for Image J.[36]

Statistical analysis

Data are presented as mean ± SD. Student's t test was used for comparison of two groups and one-way ANOVA with Dunnett's multiple comparison test for three or more groups. P values of $P < 0.05$ were considered significant.

Results

In this study, we explored the effects of perturbation of endolysosomal trafficking on exosome secretion, as previous works have shown significant changes in terms of endosomal size and number of intraluminal vesicles after knockdown of two key players in endosomal trafficking: N-Myc Downstream Regulated 1 (NDRG1)[37,38] and Ras-related protein Rab7.[30,39]

NDRG1 is a cytoplasmic protein involved in several processes including cell stress and hypoxia.[40] Recently, NDRG1 has been associated with regulation of endosomal trafficking,[41] affecting LDL receptor recycling,[38] lysosomal function[42,43] and regulation of lipid metabolism via fatty acid synthesis and exogenous uptake.[38,42,44] NDRG1 KD has been shown to increase cytoplasmic accumulation of autophagosomes,[42,43] increase lysosomal

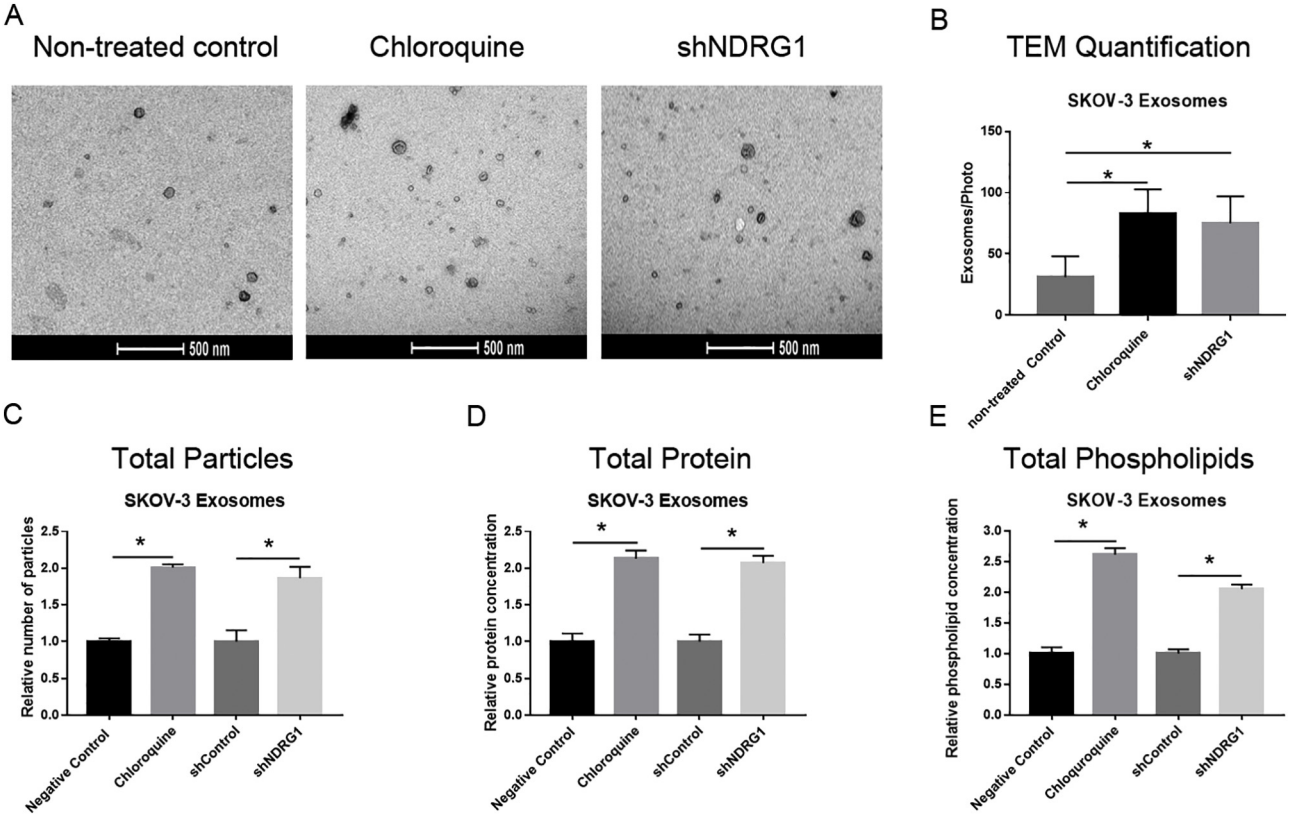

Figure 3. **Chloroquine treatment or NDRG1 knockdown increases release of exosomes.** Exosomes were isolated from 200 ml media by size exclusion chromatography. **(A)** Representative TEM pictures of exosomes obtained from treated and untreated SKOV-3 cells (scale bar represents 500 nm). **(B)** Exosome number was evaluated by TEM image quantification using ImageJ performed by an independent, blinded researcher. Bars represent mean number of vesicles per image (total of 40 pictures per condition from two independent experiments). Error bars show SD and significance is represented as * (P <0.05) as determined by Student's t test. (C) Number of particles isolated from treated or control cells as determined by nanoparticle tracking analysis (NTA). (D). Total protein levels in exosomes isolated from treated or control cells. (E) Total phospholipid levels in exosomes isolated from treated or control cells. Bars show mean of three independent experiments relative to negative control. Error bars show SD and significance is represented as * (P <0.05) as determined by Student's t test.

pH[43,45] and affect overall levels of neutral sphingolipids and ceramides.[44,45]

To evaluate effects of NDRG1 KD on the release of exosomal markers, two shRNA sequences were tested on MDA-MB-231 cells, both showing significant levels of target knockdown (Supplementary Figure 1). Cellular levels of NDRG1, exosomal marker proteins and early endosome antigen 1 (EEA1), as a marker for early endosome (EE), were also determined, as accumulation of early endosomes is a common phenomenon when endosomal trafficking is inhibited.[29,46,47] Significant reduction of ESCRT machinery components (Alix and TSG101) and EEA1 was observed for both shRNA sequences. We also evaluated viability of MDA-MB-231 cells after stable expression of either sequence, and no effects on cell survival were observed when compared with shControl transduced cells (data not shown). As both shRNA sequences showed similar effects, shNDRG1 sequence 1 was selected for follow-up experiments.

Next, we evaluated effects on exosomal marker release in three epithelial cancer cell lines (HT-29, MDA-MB-231 and SKOV-3). These cells represent varying tissues, are known to release high numbers of exosomes, and can be grown in standard cell culture conditions. NDRG1 KD was confirmed in all three cells (Figure 1, *A*, *B*). Furthermore, EAA1 and ESCRT machinery components (Alix and TSG101) levels were reduced in all three cell lines. Next, we measured exosomal markers levels in the supernatants. Exosomes were isolated from 25 ml of conditioned media by serial centrifugation, lysed and exosomal proteins were analyzed by WB. A clear increase in exosomal marker release was observed for all three cell lines after NDRG1 KD, which included not only ESCRT machinery components but also tetraspanins CD9 and CD81 (Figure 1, *C*, *D*). In addition, we evaluated whether the effect of stable NDRG1 KD on exosome release was maintained over time. Indeed, for both SKOV-3 and HT-29 cells, NDRG1 KD was found to be stable for at least 4 weeks, and the release of exosomes remained substantially increased (Supplementary Figure 2).

Rab7 is a key protein involved in multiple processes related with endosomal maturation; it is part of a Rab switch process,[47,48] where Rab5 (early endosome (EE) marker) is switched for Rab7 (late endosome (LE) marker), an essential step in LE formation and also in the transport of cargo to lysosomes.[39] In addition, Rab7 is also involved in lysosomal biogenesis and function.[49] Therefore, we next decided to assess the effects of

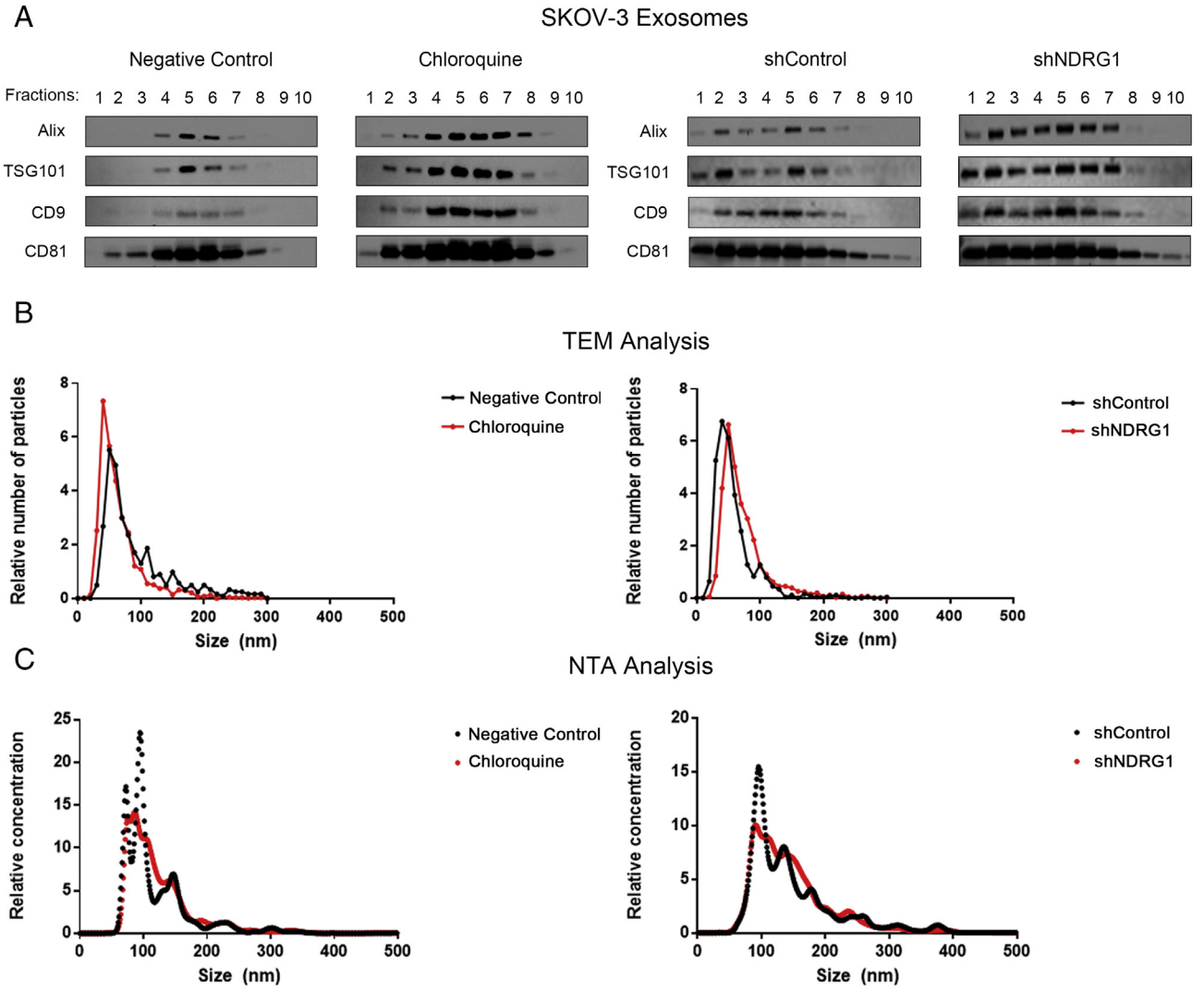

Figure 4. **Chloroquine treatment or NDRG1 knockdown does not affect exosome size distribution. (A)** Exosomes were separated into subpopulations according to size using size exclusion chromatography. 10 fractions were collected and analyzed by Western Blot. Representative Western Blots of 10 fractions of exosomes from treated or control cells are shown. **(B)** Exosome size distribution according to TEM analysis using Image J performed by an independent, blinded researcher (total of 40 pictures per condition from two independent experiments). **(C)** Exosome size distribution according to Nanoparticle tracking analysis (NTA). Graphs show mean of three independent experiments.

Rab7 KD on exosome release. First, two shRab7 sequences were tested in MDA-MB-231 cells, showing an acceptable level of KD and similar effects for both shRNA sequences (Supplementary Figure 3, *A*). Next, we determined the effect of Rab7 KD on cellular levels of ESCRT machinery components and EEA1 using WB analysis. Surprisingly, cellular levels of Alix and TSG101 were not affected by Rab7 KD using either shRNA sequence, while EEA1 was increased when compared to shControl-treated cells. shRab7 sequence 1 was selected for follow up experiments. Again, effects of Rab7 KD on exosomal marker release were next evaluated in HT-29, MDA-MB-231 and SKOV-3 cells. Rab7 KD was successful in two of these three cell types (Supplementary Figure 3, *B*), while stable expression of shRab7 was found to be toxic to SKOV-3 cells. In HT-29 and MDA-MB-231 cells, in contrast to what was seen for NDRG1 KD, cellular levels of ESCRT machinery components Alix and TSG101 were not significantly affected, while cellular EEA1 levels were found to be increased in both cell lines. The latter is suggesting cytoplasmatic accumulation of EE. Next, we measured exosome marker levels in the supernatants of Rab7 KD cells. No significant changes were observed in exosomal marker release, but, in concordance with cellular levels, a significant increment in EEA1 was observed (Supplementary Figure 3, *C*).

Next, we sought to determine whether the observed effects of increased release of exosomal markers after NDRG1 knockdown could also be achieved through inhibition of endolysosomal trafficking using chemical inhibitors. Two well-known lysosomotropic agents that efficiently inhibit endosomal maturation were selected: chloroquine and NH_4Cl. Both agents accumulate

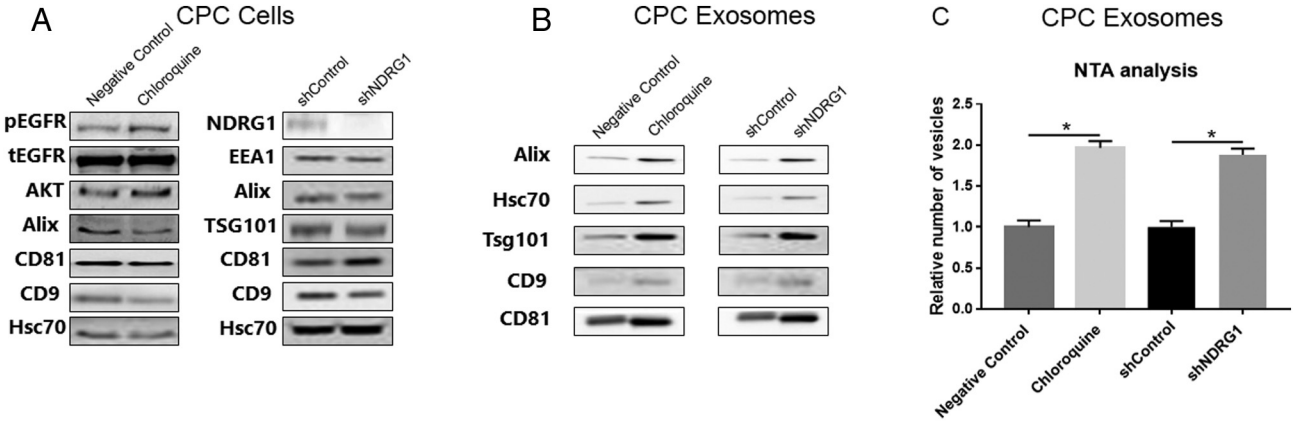

Figure 5. **Chloroquine treatment or NDRG1 knockdown increases release of exosomes from cardiac progenitor cells. (A)** Representative Western Blot of treated and untreated CPCs. Equal protein amounts were loaded. **(B)** Exosomes were isolated by serial centrifugation from media of treated or control cells. Exosomal marker protein levels were analyzed by Western Blot. Equal volumes were loaded. **(C)** Number of particles isolated from treated or control cells as determined by nanoparticle tracking analysis (NTA). Bars show mean of three independent experiments relative to control (negative control for chloroquine treated cells and shControl for NDRG1 KD cells). Error bars show SD and significance is represented as * (P <0.05) as determined by Student's t test.

inside the acidic compartments of treated cells, including endosomes and lysosomes, leading to inhibition of lysosomal enzymes, which require an acidic pH, and preventing fusion of endosomes and lysosomes.[50,51]

First, we evaluated the optimal concentration of both agents for a 24 h incubation period, according to literature[52] and experimental evaluation. The optimal concentrations were found to be 20 μg/ml for chloroquine and 2 mM for NH_4Cl (data not shown). Next, we measured release of exosomal markers by untreated, chloroquine treated and NH_4Cl treated cells. Exosomes were again isolated from 25 ml of conditioned media by serial centrifugation, lysed and protein expressions analyzed by WB. Quantification showed an increased release of the four exosomal markers Alix, TSG101, CD9 and CD81 in supernatants from all three cell lines after either treatment, confirming that interfering with endolysosomal trafficking stimulates release of exosomal proteins (Figure 2, *A*, *B*).

To confirm that NDRG1 KD and chloroquine treatment indeed affected endosomal maturation in our system, an acridine orange (AO) assay was performed in SKOV-3 cells. AO is a cell permeable fluorophore that is protonated and thereby becomes trapped in acidic vesicles or organelles. OA fluorescence is green at low concentrations (520 nm), but at high concentrations, as obtained in acidic endosomes, AO fluorescence is shifted to red fluorescence (620 nm). Confocal analysis of acridine orange stained cells showed a decrease in red fluorescence in NDRG1 KD and chloroquine treated cells, confirming inhibition of lysosomal acidification (Supplementary Figure 4).

We next aimed to determine if the observed increased release of exosomal markers was due to a higher recruitment of exosomal markers on the vesicles or due to an increase in the total number of exosomal particles. For this reason, several experiments were performed to quantify release of exosome particles. We switched to established size exclusion chromatography protocols[25,53] for exosome isolation for these experiments, as differential ultracentrifugation has been shown to affect exosome integrity and functionality.[25,54] The UV chromatograms obtained during SEC isolation showed higher absorbance values in the EV fractions (elution volumes 40-50 ml) of samples from NDRG1 KD and chloroquine-treated cells as compared to shControl and untreated cells, respectively (Supplementary Figure 5), indicating an increase in exosome release.

After SEC, exosome-containing fractions were concentrated and used for further analysis. Quantification of TEM images showed an approximately 2-fold increase of vesicles in treated samples compared with control samples (Figure 3, *A*, *B* and Supplementary Figure 6). In concordance with these results, exosomal particle (Figure 3, *C*), protein (Figure 3, *D*) and phospholipid levels (Figure 3, *E*) were increased to a similar extent. Moreover, exosomes released from NDRG1 KD and shControl cells showed similar levels of enrichment for exosome marker proteins CD81 and TSG101, a similar level of depletion of β-actin, and absence of endoplasmatic reticulum marker protein Calnexin (Supplementary Figure 7). These results show that, while the number of particles is significantly increased by either treatment, total protein and total phospholipid levels per exosome are not affected, suggesting similar overall exosomal cargo levels.

As cells have been shown to release distinct subpopulations of exosomes and these subpopulations differ in size,[55] we next assessed the size distribution of exosomes obtained from NDRG1 KD and chloroquine treated cells. An altered size distribution could highlight the enrichment of specific exosomal subpopulations. For this reason, size distribution was evaluated in detail by three different methods. First, isolated exosomes were loaded on a size exclusion column packed with Sephacryl S-1000, which allows separation of exosome subpopulations based on size,[55] and separated into 10 fractions. Exosome subpopulations were pelleted at 200,000 ×g using ultracentrifugation and analyzed by WB for exosomal markers Alix, TSG101, CD9 and CD81. While the total levels of these marker proteins increased after NDRG1 KD or chloroquine treatment, no significant differences were observed in their

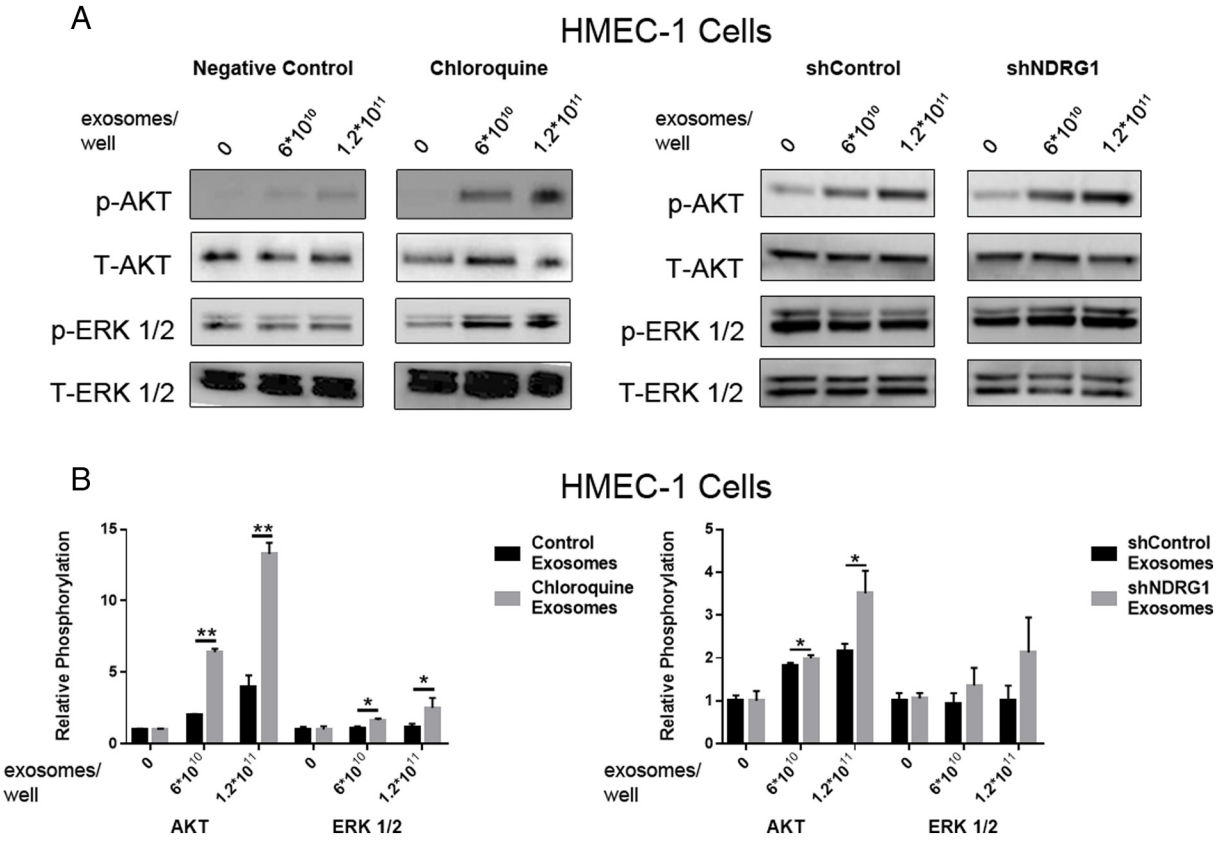

Figure 6. **Exosomes from treated cells increase AKT and ERK 1/2 phosphorylation in endothelial cells.** Exosomes were isolated by size exclusion chromatography, quantified and added to HMEC-1 cells at increasing concentrations. HMEC-1 cells were incubated for 30 min. **(A)** Representative Western Blot showing levels of phosphorylated AKT and ERK 1/2 in cells after incubation with exosomes from treated or control cells. **(B)** Quantification of AKT and ERK 1/2 phosphorylation. Band intensities were determined using ImageJ software. Phosphorylation is expressed as relative ratio between phosphorylated and total AKT or ERK 1/2. Bars represent mean of three independent experiments. Error bars show SD and significance is represented as * (P <0.05) or ** (P <0.005) as determined by Student's t test.

relative distribution over different fractions (Figure 4, *A*). Furthermore, analysis of exosome preparations by TEM and NTA analysis did not reveal major differences in size distribution (Figure 4, *B*, *C*). Thus, NDRG1 KD and chloroquine treatments do not seem to stimulate release of a single specific exosome subpopulation.

After evaluating the effects of NDRG1 KD and chloroquine on release of exosomes by tumor cells, we sought to evaluate the functionality of these exosomes for translational purposes, e.g. for regenerative medicine applications. While cell therapy using stem or progenitor cells has been shown to be a promising approach to stimulate tissue regeneration, it has the risk of unwanted transformations and/or genetic changes of the cells before and after transplantation. According to multiple reports, the effect of stem/progenitor cell transplantation on tissue regeneration is due to paracrine stimulation of resident cells, including via exosomes.[24,56] Therefore, cell-free regenerative medicine strategies using exosomes derived from stem or progenitor cells is a promising alternative to cell transplantation. Recently, exosomes from CPCs have been demonstrated to have therapeutic efficacy in rodent models of myocardial ischemia and ischemia/reperfusion injury.[57] Mechanistically, CPC-derived exosomes induce pro-survival pathways and angiogenesis in endothelial cells,[58] and protect against cardiomyocyte apoptosis.[59] For this reason, we evaluated the effects of NDRG1 KD and chloroquine on release of exosomes by CPCs.

First, NDRG1 KD was confirmed to be successful in CPCs. Both NDRG1 and chloroquine treatment reduced cellular levels of Alix (Figure 5, *A*). Next, we measured exosomal markers levels in the supernatants of CPCs. An increment in exosomal marker release was observed in conditioned media from NDRG1 KD cells compared with media from shControl transduced cells. Also, for chloroquine treated cells, a substantially increased release of exosomal marker proteins was observed (Figure 5, *B*). Finally, NTA analysis was performed for exosomes isolated from media from NDRG1 KD, chloroquine treated and control cells. Again, a two-fold increase in particle number was observed for treated cells as compared to controls.

CPC-derived exosomes have been previously shown to activate AKT and ERK1/2 pathways in target cells.[21,58–60] These pathways play an important role in cell survival, migration and angiogenesis of endothelial cells. To investigate whether exosomes from NDRG1 KD or chloroquine treated cells retain their bioactivity in tissue repair, HMEC-1 and HL-1

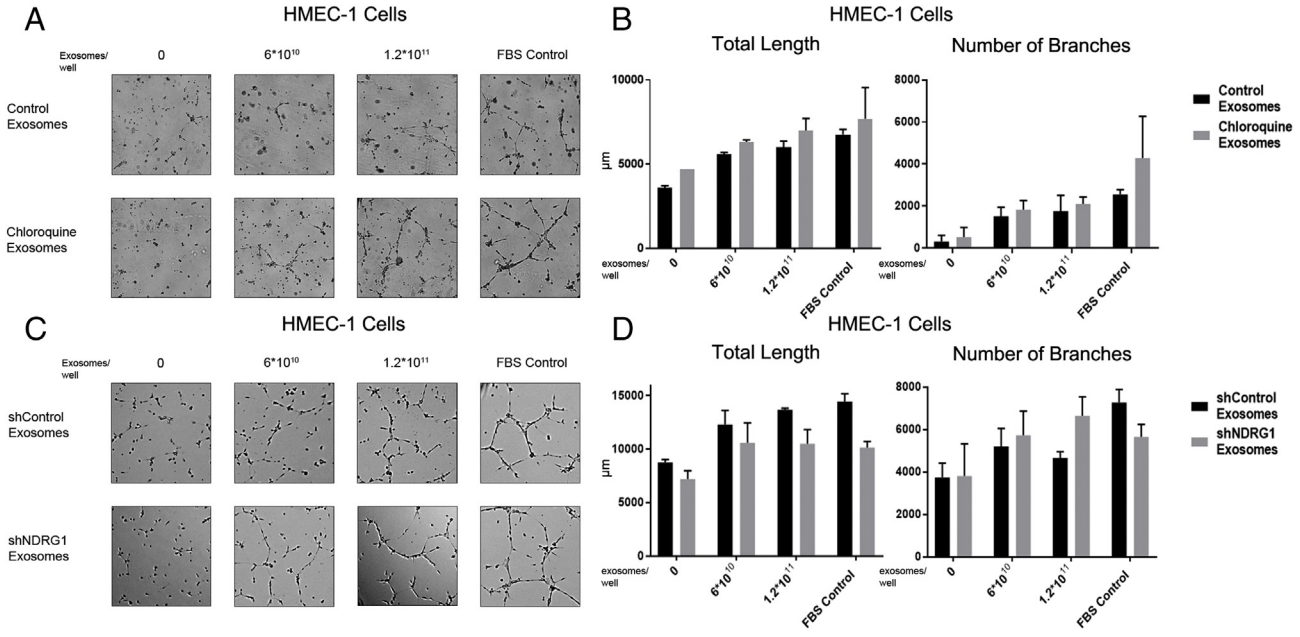

Figure 7. **Exosomes from treated cells induce angiogenesis in HMEC-1 cells.** HMEC-1 cells were pre-incubated with increasing concentrations of exosomes for 12 h. Then, equal numbers of cells were seeded onto Matrigel, and pictures were taken after 7 h. **(A, C)** Representative pictures of tube formation by treated or control HMEC-1 cells. **(B, D)** Quantification of angiogenesis was performed using the angiogenesis analyzer tool from Image J. Graphs represent quantification of total tube length of and total number of branches. Data are represented as mean of two independent experiments.

cells were stimulated with equal numbers of exosomes from treated or control CPCs. In HMEC-1 cells, a dose dependent increase in AKT and ERK1/2 phosphorylation was observed for exosomes from all conditions. Interestingly, a significantly higher level of phosphorylation was observed for exosomes from NDRG1 KD or chloroquine treated cells as compared to control cells (Figure 6, *A*, *B*). HL-1 cells only showed activation of phosphorylation of ERK1/2 in response to CPC-exosome treatment. (Supplementary Figure 8).

Finally, as CPC exosomes were previously described to stimulate angiogenesis, a tube formation assay with HMEC-1 cells was performed in order to assess angiogenic stimulation of exosomes from treated and control CPCs. Cells were pre-incubated with an equal number of exosomes for 12 h in the absence of serum, after which they were seeded onto Matrigel. After 7 h incubation, pictures were taken and total tubule length and number of branches was assessed by Image J angiogenesis analysis.[36] A clear increase in total tube length and number of branches was observed in cells treated with either NDRG1 KD or chloroquine treated cell-derived exosomes or control CPC-derived exosomes (Figure 7). No significant differences in angiogenesis stimulation were observed between the different treatments. Together, these data indicate that the pro-angiogenic bioactivity of exosomes from NDRG1 KD or chloroquine-treated CPCs is retained.

Discussion

Application of exosomes from stem- or progenitor cells has been demonstrated to be a promising new treatment for tissue regeneration. Progenitor cells possess high growth rates and differentiation capacity. When exosomes from cells are taken up by the target cells, they transmit new characteristics, such as pro-survival effects, growth stimulation, migratory capacity and, as also shown in this work, activation of signaling pathways and angiogenesis. Exosome-mediated transmission of cell characteristics is a complex process that includes transference of an untold number of miRNAs and proteins with specific functions, as described in a large number of previous studies.[61–64] In addition, exosomes from both primary cultures and cell lines have been employed for delivery of different kinds of therapeutic agents including small molecular drugs, RNA and proteins for the treatment of cancer, septic shock, inflammatory conditions and neurodegenerative disease.[65,66] Unfortunately, exosomes' therapeutic effects are typically only obtained when target tissues are stimulated with concentrations of exosomes that exceed physiological concentrations. For this reason, one of the limitations of exosome-based therapy is the necessity to grow a very large number of cells to produce enough exosomes to treat an injured tissue or organism.[17]

Exosomes originate from ILVs inside MVEs. The fate of MVEs is either fusion with lysosomes, resulting in degradation of their content, or fusion with the plasma membrane, releasing ILVs as exosomes. Therefore, we hypothesized that interfering with endolysosomal trafficking would stimulate exosome release. While a few studies have previously suggested a link between abnormalities in endosomal maturation or lysosomal function and release of exosomes,[67,68] we, to the best of our knowledge, are the first to determine functionality of these exosomes for further application in the field of regenerative medicine. Here, we demonstrate a strategy to disrupt endolysosomal maturation, which results in a two-fold increase in

exosome yield, and show that this strategy does not affect their bioactivity.

We first targeted two known players in endosomal trafficking, NDRG1 and Rab7, by RNA interference technology, with the aims to evaluate the effect of knockdown of these proteins on the release of exosomes. NDRG1 is known to be involved in lysosomal stability and endosome recycling,[38,43] while RAB7 is one of the most studied proteins involved in the regulation of endosomal trafficking.[30,48] We observed that NDRG1 KD decreased cellular levels of components of the ESCRT machinery, in concordance with a previous report of Pietianem et al.[38] Next, we observed for first time that this reduction was accompanied by an increment in the release of exosomes. It is important to highlight that NDRG1 KD not just reduces lysosomal function, but may also induce an increment of neutral sphingolipids and ceramides,[38,44] which are known to affect exosome biogenesis.[69] Then, in opposition to what we expected and other authors have suggested,[70] Rab7 KD did not affect exosome release. Rab7 KD did not affect cellular levels of the ESCRT proteins Alix and TSG101, but increased the level of EEA1 in cells and exosomes, suggesting accumulation of EE and enhanced release of an ILV/exosome population produced during early steps of endosomal maturation or when the EEA1 marker is still present.

We also tested whether two well-known lysosomotropic agents, chloroquine and NH_4Cl, could increase exosome release and obtained very similar results as for NDRG1 KD; these observations suggest that the lysosomotropic effect of NDRG1 KD is responsible for the observed increased exosome production.

To evaluate the translational potential of our strategy we next evaluated the effect of lysosomotropic treatments on the size, cargo and bioactivity of exosomes. Our analyses revealed no significant changes in exosome size, protein to particle ratio or protein to (phospho)lipid ratio upon treatment. However, changes in exosome composition cannot be ruled out and require further detailed studies. In terms of lipid cargo, enrichment of ceramides and neutral sphingolipids as a result of NDRG1 KD[38,44] could affect the release of exosomes with different cargo due to curvature increment. Furthermore, although in our work we did not observe consistent variations in levels of exosomal marker proteins, it was reported before that the treatment of Bafilomycin A, a drug that neutralizes the lysosomal pH, affects the exosome protein composition.[71] Therefore, we finally set out to evaluate functionality of exosomes obtained after treatment.

Through in vitro experiments, we tested bioactivity of obtained exosomes by evaluating their ability to activate AKT and ERK1/2 pathways in endothelial cells and cardiomyocytes, as well as by tube formation assays to simulate angiogenesis induction. We have previously shown that CPC-derived exosomes reduce cardiac damage after myocardial infarction through activation of AKT and ERK1/2 pathways, involved in cell survival and proliferation, and stimulation of angiogenesis.[25,57,58] Encouragingly, exosomes derived from NDRG1 KD and chloroquine treated CPCs increased phosphorylation of AKT and ERK1/2 and induced angiogenesis to at least the same extent as normal CPC-derived exosomes, suggesting that their bioactivity is retained.

In conclusion, this report shows that targeting of a single protein, NDRG1, can significantly increase the release of functional exosomes. To our knowledge, this is the first time that NDRG1 has been demonstrated to affect exosome release. NDRG1 KD strategy could be applied as a tool for biological studies of cell–cell interactions via exosomes. We also show that the stimulatory effects can be mimicked using small molecular compounds chloroquine and NH_4Cl, which may offer a straightforward approach to boost exosome production under regular cell culture conditions. The employment of these chemical treatments could significantly reduce time, space and costs in the production of therapeutic exosomes.

Altogether, our study contributes to the general knowledge in the field of exosomes, and may be employed either as a tool for the understanding biological processes in which exosomes are involved or as a strategy to facilitate clinical translation of exosome therapeutics by increasing their production.

Appendix A. Supplementary data

Supplementary data to this article can be found online at https://doi.org/10.1016/j.nano.2019.102014.

References

1. Théry C, Zitvogel L, Amigorena S. Exosomes: composition, biogenesis and function. *Nat Rev Immunol* 2002;**2**(8):569-79, https://doi.org/10.1038/nri855.
2. Challagundla KB, Wise PM, Neviani P, et al. Exosome-mediated transfer of microRNAs within the tumor microenvironment and neuroblastoma resistance to chemotherapy. *J Natl Cancer Inst* 2015;**107**(7), https://doi.org/10.1093/jnci/djv135.
3. Zhang X, Yuan X, Shi H, Wu L, Qian H, Xu W. Exosomes in cancer: small particle, big player. *J Hematol Oncol* 2015;**8**83, https://doi.org/10.1186/s13045-015-0181-x.
4. Martins VR, Dias MS, Hainaut P. Tumor-cell-derived microvesicles as carriers of molecular information in cancer. *Curr Opin Oncol* 2013;**25**(1):66-75, https://doi.org/10.1097/CCO.0b013e32835b7c81.
5. Peinado H, Alečković M, Lavotshkin S, et al. Melanoma exosomes educate bone marrow progenitor cells toward a pro-metastatic phenotype through MET. *Nat Med* 2012;**18**(6):883-91, https://doi.org/10.1038/nm.2753.
6. Peinado H, Lavotshkin S, Lyden D. The secreted factors responsible for pre-metastatic niche formation: old sayings and new thoughts. *Semin Cancer Biol* 2011;**21**(2):139-46, https://doi.org/10.1016/j.semcancer.2011.01.002.
7. Fader CM, Savina A, Sánchez D, Colombo MI. Exosome secretion and red cell maturation: exploring molecular components involved in the docking and fusion of multivesicular bodies in K562 cells. *Blood Cells Mol Dis* 2005;**35**(2):153-7http://www.ncbi.nlm.nih.gov/pubmed/16099697.
8. Greening DW, Gopal SK, Xu R, Simpson RJ, Chen W. Exosomes and their roles in immune regulation and cancer. *Semin Cell Dev Biol* 2015;**40**:72-81, https://doi.org/10.1016/j.semcdb.2015.02.009.
9. Huber HJ, Holvoet P. Exosomes: emerging roles in communication between blood cells and vascular tissues during atherosclerosis. *Curr Opin Lipidol* 2015;**26**(5):412-9, https://doi.org/10.1097/MOL.0000000000000214.
10. Yin M, Loyer X, Boulanger CM. Extracellular vesicles as new pharmacological targets to treat atherosclerosis. *Eur J Pharmacol* July 2015, https://doi.org/10.1016/j.ejphar.2015.06.047.

11. Todorova D, Simoncini S, Lacroix R, Sabatier F, Dignat-George F. Extracellular vesicles in angiogenesis. *Circ Res* 2017;**120**(10):1658-73, https://doi.org/10.1161/CIRCRESAHA.117.309681.
12. Minciacchi VR, Freeman MR, Di Vizio D. Extracellular vesicles in cancer: exosomes, microvesicles and the emerging role of large oncosomes. *Semin Cell Dev Biol* 2015;**40**:41-51, https://doi.org/10.1016/j.semcdb.2015.02.010.
13. Wu X, Zheng T, Zhang B. Exosomes in Parkinson's disease. *Neurosci Bull* 2017;**33**(3):331-8, https://doi.org/10.1007/s12264-016-0092-z.
14. Deddens JC, Vrijsen KR, Colijn JM, et al. Circulating extracellular vesicles contain miRNAs and are released as early biomarkers for cardiac injury. *J Cardiovasc Transl Res* 2016;**9**(4):291-301, https://doi.org/10.1007/s12265-016-9705-1.
15. Ellwanger JH, Veit TD, Chies JAB. Exosomes in HIV infection: a review and critical look. *Infect Genet Evol* 2017;**53**:146-54, https://doi.org/10.1016/j.meegid.2017.05.021.
16. Liu Y, Li D, Liu Z, et al. Targeted exosome-mediated delivery of opioid receptor Mu siRNA for the treatment of morphine relapse. *Sci Rep* 2015;**5**(1)17543, https://doi.org/10.1038/srep17543.
17. Yamashita T, Takahashi Y, Takakura Y. Possibility of exosome-based therapeutics and challenges in production of exosomes eligible for therapeutic application. *Biol Pharm Bull* 2018;**41**(6):835-42, https://doi.org/10.1248/bpb.b18-00133.
18. Bunggulawa EJ, Wang W, Yin T, et al. Recent advancements in the use of exosomes as drug delivery systems. *J Nanobiotechnology* 2018;**16**(1):81, https://doi.org/10.1186/s12951-018-0403-9.
19. Vader P, Mol EA, Pasterkamp G, Schiffelers RM. Extracellular vesicles for drug delivery. *Adv Drug Deliv Rev* 2016;**106**:148-56, https://doi.org/10.1016/j.addr.2016.02.006 Pt A.
20. Kourembanas S. Exosomes: vehicles of intercellular signaling, biomarkers, and vectors of cell therapy. *Annu Rev Physiol* 2015;**77**:13-27, https://doi.org/10.1146/annurev-physiol-021014-071641.
21. Ibrahim AG-E, Cheng K, Marbán E. Exosomes as critical agents of cardiac regeneration triggered by cell therapy. *Stem Cell Reports* 2014;**2**(5):606-19, https://doi.org/10.1016/j.stemcr.2014.04.006.
22. Sun D, Zhuang X, Xiang X, et al. A novel nanoparticle drug delivery system: the anti-inflammatory activity of curcumin is enhanced when encapsulated in exosomes. *Mol Ther* 2010;**18**(9):1606-14, https://doi.org/10.1038/mt.2010.105.
23. Batrakova EV, Kim MS. Using exosomes, naturally-equipped nanocarriers, for drug delivery. *J Control Release* 2015;**219**:396-405, https://doi.org/10.1016/j.jconrel.2015.07.030.
24. Sluijter JPG, Davidson SM, Boulanger CM, et al. Extracellular vesicles in diagnostics and therapy of the ischaemic heart: position paper from the working group on cellular biology of the heart of the European Society of Cardiology. *Cardiovasc Res* 2018;**114**(1):19-34, https://doi.org/10.1093/cvr/cvx211.
25. Mol EA, Goumans M-J, Doevendans PA, Sluijter JPG, Vader P. Higher functionality of extracellular vesicles isolated using size-exclusion chromatography compared to ultracentrifugation. *Nanomedicine Nanotechnology, Biol Med* 2017;**13**(6):2061-5, https://doi.org/10.1016/j.nano.2017.03.011.
26. Scott CC, Vacca F, Gruenberg J. Endosome maturation, transport and functions. *Semin Cell Dev Biol* 2014;**31**:2-10, https://doi.org/10.1016/j.semcdb.2014.03.034.
27. Hessvik NP, Llorente A. Current knowledge on exosome biogenesis and release. *Cell Mol Life Sci* 2018;**75**(2):193-208, https://doi.org/10.1007/s00018-017-2595-9.
28. Ostrowski M, Carmo NB, Krumeich S, et al. Rab27a and Rab27b control different steps of the exosome secretion pathway. *Nat Cell Biol* 2010;**12**(1):19-30 sup pp 1–13https://doi.org/10.1038/ncb2000.
29. Huotari J, Helenius A. Endosome maturation. *EMBO J* 2011;**30**(17):3481-500, https://doi.org/10.1038/emboj.2011.286.
30. Vanlandingham PA, Ceresa BP. Rab7 regulates late endocytic trafficking downstream of multivesicular body biogenesis and cargo sequestration *. 2009. doi:https://doi.org/10.1074/jbc.M809277200
31. Vrijsen KR, Sluijter JPG, Schuchardt MWL, et al. Cardiomyocyte progenitor cell-derived exosomes stimulate migration of endothelial cells. *J Cell Mol Med* 2010;**14**(5), https://doi.org/10.1111/j.1582-4934.2010.01081.x.
32. Tschan MP, Shan D, Laedrach J, et al. NDRG1/2 expression is inhibited in primary acute myeloid leukemia. *Leuk Res* 2010;**34**(3):393-8, https://doi.org/10.1016/j.leukres.2009.08.037.
33. Alonso-Curbelo D, Osterloh L, Cañón E, et al. RAB7 counteracts PI3K-driven macropinocytosis activated at early stages of melanoma development. *Oncotarget* 2015;**6**(14):11848-62, https://doi.org/10.18632/oncotarget.4055.
34. Schneider CA, Rasband WS, Eliceiri KW. NIH Image to ImageJ: 25 years of image analysis. *Nat Methods* 2012;**9**(7):671-5, https://doi.org/10.1038/nmeth.2089.
35. Rouser G, Fleischer S, Yamamoto A. Two dimensional thin layer chromatographic separation of polar lipids and determination of phospholipids by phosphorus analysis of spots. *Lipids* 1970;**5**(5):494-6, https://doi.org/10.1007/BF02531316.
36. Gilles Carpentier. Angiogenesis analyzer for ImageJ [ImageJ User and Developer Conference]. http://imagejconf.tudor.lu/program/poster/gilles_carpentier1748951862. Accessed December 29, 2018.
37. Askautrud HA, Gjernes E, Gunnes G, et al. Global gene expression analysis reveals a link between NDRG1 and vesicle transport. Rishi A, ed. *PLoS One*. 2014;9(1):e87268. doi:https://doi.org/10.1371/journal.pone.0087268
38. Pietiainen V, Vassilev B, Blom T, et al. NDRG1 functions in LDL receptor trafficking by regulating endosomal recycling and degradation. *J Cell Sci* 2013;**126**(17):3961-71, https://doi.org/10.1242/jcs.128132.
39. Feng Y, Press B, Wandinger-Ness A. Rab 7: an important regulator of late endocytic membrane traffic. J Cell Biol 1995;131(6 Pt 1):1435–1452. http://www.ncbi.nlm.nih.gov/pubmed/8522602. Accessed October 22, 2018.
40. Said HM, Safari R, Al-Kafaji G, et al. Time- and oxygen-dependent expression and regulation of NDRG1 in human brain cancer cells. *Oncol Rep* 2017;**37**(6):3625-34, https://doi.org/10.3892/or.2017.5620.
41. Askautrud HA, Gjernes E, Gunnes G, et al. Global gene expression analysis reveals a link between NDRG1 and vesicle transport. *PLoS One* 2014;**9**(1)e87268, https://doi.org/10.1371/journal.pone.0087268.
42. Sahni S, Bae D-H, Lane DJR, et al. The metastasis suppressor, N-myc downstream-regulated gene 1 (NDRG1), inhibits stress-induced autophagy in cancer cells. *J Biol Chem* 2014;**289**(14):9692-709, https://doi.org/10.1074/jbc.M113.529511.
43. Wang H, Li W, Xu J, et al. NDRG1 inhibition sensitizes osteosarcoma cells to combretastatin A-4 through targeting autophagy. *Cell Death Dis* 2017;**8**(9)e3048, https://doi.org/10.1038/cddis.2017.438.
44. Sevinsky CJ, Khan F, Kokabee L, Darehshouri A, Maddipati KR, Conklin DS. NDRG1 regulates neutral lipid metabolism in breast cancer cells. *Breast Cancer Res* 2018;**20**(1):55, https://doi.org/10.1186/s13058-018-0980-4.
45. Pietiäinen V, Vassilev B, Blom T, et al. NDRG1 functions in LDL receptor trafficking by regulating endosomal recycling and degradation. 2013;**126**(17)http://jcs.biologists.org/content/126/17/3961.short.
46. Press B, Feng Y, Hoflack B, Wandinger-Ness A. Mutant Rab7 causes the accumulation of cathepsin D and cation-independent mannose 6–phosphate receptor in an early endocytic compartment. *J Cell Biol* 1998;**140**(5):1075-89, https://doi.org/10.1083/JCB.140.5.1075.
47. Rink J, Ghigo E, Kalaidzidis Y, Zerial M. Rab conversion as a mechanism of progression from early to late endosomes. *Cell* 2005;**122**(5):735-49, https://doi.org/10.1016/J.CELL.2005.06.043.
48. Guerra F, Bucci C. Multiple roles of the small GTPase Rab7. *Cell* 2016;**5**(3), https://doi.org/10.3390/cells5030034.
49. Bucci C, Thomsen P, Nicoziani P, McCarthy J, van Deurs B. Rab7: a key to lysosome biogenesis. *Mol Biol Cell* 2000;**11**(2):467-80, https://doi.org/10.1091/mbc.11.2.467.
50. Rutz M, Metzger J, Gellert T, et al. Toll-like receptor 9 binds single-stranded CpG-DNA in a sequence- and pH-dependent manner. *Eur J Immunol* 2004;**34**(9):2541-50, https://doi.org/10.1002/eji.200425218.

51. De Duve C, De Barsy T, Poole B, Trouet A, Tulkens P, Van Hoof F. Lysosomotropic agents. *Biochem Pharmacol* 1974;**23**(18):2495-531, https://doi.org/10.1016/0006-2952(74)90174-9.
52. Misinzo G, Delputte PL, Nauwynck HJ, et al. Inhibition of endosome-lysosome system acidification enhances porcine circovirus 2 infection of porcine epithelial cells recently. Misinzo et al.*G J Virol* 2008;**82**(3):1128-35, https://doi.org/10.1128/JVI.01229-07.
53. Nordin JZ, Lee Y, Vader P, et al. Ultrafiltration with size-exclusion liquid chromatography for high yield isolation of extracellular vesicles preserving intact biophysical and functional properties. *Nanomedicine Nanotechnology, Biol Med* 2015;**11**(4):879-83, https://doi.org/10.1016/j.nano.2015.01.003.
54. Linares R, Tan S, Gounou C, Arraud N, Brisson AR. High-speed centrifugation induces aggregation of extracellular vesicles. *J Extracell vesicles* 2015;**4**29509, https://doi.org/10.3402/jev.v4.29509.
55. Willms E, Johansson HJ, Mäger I, et al. Cells release subpopulations of exosomes with distinct molecular and biological properties. *Sci Rep* 2016;**6**(1)22519, https://doi.org/10.1038/srep22519.
56. Anthony DF, Shiels PG. Exploiting paracrine mechanisms of tissue regeneration to repair damaged organs. *Transplant Res* 2013;**2**(1):10, https://doi.org/10.1186/2047-1440-2-10.
57. Maring JA, Lodder K, Mol E, et al. Cardiac progenitor cell–derived extracellular vesicles reduce infarct size and associate with increased cardiovascular cell proliferation. *J Cardiovasc Transl Res* November 2018, https://doi.org/10.1007/s12265-018-9842-9.
58. Vrijsen KR, Maring JA, Chamuleau SAJ, et al. Exosomes from cardiomyocyte progenitor cells and mesenchymal stem cells stimulate angiogenesis via EMMPRIN. *Adv Healthc Mater* 2016;**5**(19):2555-65, https://doi.org/10.1002/adhm.201600308.
59. Xiao J, Pan Y, Li XH, et al. Cardiac progenitor cell-derived exosomes prevent cardiomyocytes apoptosis through exosomal miR-21 by targeting PDCD4. *Cell Death Dis* 2016;**7**(6):e2277, https://doi.org/10.1038/cddis.2016.181.
60. Andriolo G, Provasi E, Lo Cicero V, et al. Exosomes from human cardiac progenitor cells for therapeutic applications: development of a GMP-grade manufacturing method. *Front Physiol* 2018;**9**1169, https://doi.org/10.3389/fphys.2018.01169.
61. Zhang Z, Li X, Sun W, et al. Loss of exosomal miR-320a from cancer-associated fibroblasts contributes to HCC proliferation and metastasis. *Lett* 2017;**397**:33-42, https://doi.org/10.1016/j.canlet.2017.03.004.
62. Greither T, Grochola LF, Udelnow A, Lautenschläger C, Würl P, Taubert H. Elevated expression of microRNAs 155, 203, 210 and 222 in pancreatic tumors is associated with poorer survival. *Int J Cancer* 2010;**126**(1):73-80, https://doi.org/10.1002/ijc.24687.
63. Berchem G, Noman MZ, Bosseler M, et al. Hypoxic tumor-derived microvesicles negatively regulate NK cell function by a mechanism involving TGF-β and miR23a transfer. *Oncoimmunology* 2016;**5**(4) e1062968, https://doi.org/10.1080/2162402X.2015.1062968.
64. Yin Y, Cai X, Chen X, et al. Tumor-secreted miR-214 induces regulatory T cells: a major link between immune evasion and tumor growth. *Cell Res* 2014;**24**(10):1164-80, https://doi.org/10.1038/cr.2014.121.
65. Wang J, Zheng Y, Zhao M. Exosome-based cancer therapy: implication for targeting cancer stem cells. *Front Pharmacol* 2016;**7**:533, https://doi.org/10.3389/fphar.2016.00533.
66. Luan X, Sansanaphongpricha K, Myers I, Chen H, Yuan H, Sun D. Engineering exosomes as refined biological nanoplatforms for drug delivery. *Acta Pharmacol Sin* 2017;**38**(6):754-63, https://doi.org/10.1038/aps.2017.12.
67. Yuyama K, Yamamoto N, Yanagisawa K. Accelerated release of exosome-associated GM1 ganglioside (GM1) by endocytic pathway abnormality: another putative pathway for GM1-induced amyloid fibril formation. J Neurochem doi:https://doi.org/10.1111/j.1471-4159.2007.05128.x
68. Miranda AM, Lasiecka ZM, Xu Y, et al. Neuronal lysosomal dysfunction releases exosomes harboring APP C-terminal fragments and unique lipid signatures. *Nat Commun* 2018;**9**(1):291, https://doi.org/10.1038/s41467-017-02533-w.
69. Trajkovic K, Hsu C, Chiantia S, et al. Ceramide triggers budding of exosome vesicles into multivesicular endosomes. *Science (80)*. 2008;319(5867). http://science.sciencemag.org/content/319/5867/1244?ijkey=57436599aa8999d70fda19d27dfe1808d27d9016bf&keytype2=tf_ipsecsha. Accessed June 6, 2017.
70. Eitan E, Suire C, Zhang S, Mattson MP. Impact of lysosome status on extracellular vesicle content and release. *Ageing Res Rev* 2016;**32**:65-74, https://doi.org/10.1016/j.arr.2016.05.001.
71. Alvarez-Erviti L, Seow Y, Schapira AH, et al. Lysosomal dysfunction increases exosome-mediated alpha-synuclein release and transmission. *Neurobiol Dis* 2011;**42**(3):360-7, https://doi.org/10.1016/j.nbd.2011.01.029.